Evidence for a spin pseudogap in the normal state of superconducting Mo_3Sb_7

2009 J. Phys.: Condens. Matter 21 485701

(http://iopscience.iop.org/0953-8984/21/48/485701)

J. Phys.: Condens. Matter **21** (2009) 485701 (7pp) doi:10.1088/0953-8984/21/48/485701

Evidence for a spin pseudogap in the normal state of superconducting Mo_3Sb_7

V H Tran[1], A D Hillier[2], D T Adroja[2], Z Bukowski[3] and W Miiller[1]

[1] Institute of Low Temperature and Structure Research, Polish Academy of Sciences, PO Box 1410, 50-950 Wrocław, Poland
[2] ISIS Facility, Rutherford Appleton Laboratory, Chilton, Oxfordshire OX11 0QX, UK
[3] Laboratory for Solid State Physics, ETH Zürich, 8093 Zürich, Switzerland

Received 26 April 2009, in final form 6 October 2009
Published 30 October 2009
Online at stacks.iop.org/JPhysCM/21/485701

Abstract

Using muon spin relaxation (μSR) and inelastic neutron scattering (INS) we have investigated the normal state of the superconductor Mo_3Sb_7 and the reference compound Ru_3Sn_7. The μSR experiments on Ru_3Sn_7 reveal static and relatively slow dynamic relaxations, which are ascribed to a random static nuclear dipole field and thermally activated muon motion, respectively. INS experiments on Ru_3Sn_7, on the other hand, reveal three phononic excitations at 11, 18 and 23 meV, substantiating the assertion of Einstein and Debye oscillations derived from the specific heat and electrical resistivity data. The distinct difference in the μSR as well as INS spectra between Ru_3Sn_7 and Mo_3Sb_7 provides strong evidence for a magnetic/electronic nature of the phase transition at $T^* = 50$ K in the Mo-based compound. On the basis of the μSR and INS data, the energy spin pseudogap of 150(10) K was estimated. The observed weak magnetism in the dynamic susceptibility $\chi''(Q, \omega)$ and residual longitudinal field relaxation at 5 K imply a static ordering or quantum fluctuations.

(Some figures in this article are in colour only in the electronic version)

1. Introduction

In conventional BCS superconductors, the phonon-mediated pairing is believed to be the principle mechanism. Thus, any non-phonon interaction tends to decrease the superconducting temperature in BCS systems. On the contrary, in unconventional superconductors, including high-Tc cuprates and heavy-fermion, an electron–electron correlation acts as a magnetic glue very similar to phonons in BCS and enhances the superconductivity [1]. The consequence being that some unconventional superconductors, before undergoing into a superconducting state have shown a transition which is magnetic in nature at higher temperatures. Such a transition may be antiferromagnetic (for instance in UPd_2Al_3, UNi_2Al_3) [2], ferromagnetic (UGe_2, URhGe) [3], or even a (pseudo) spin/charge-gap type (underdoped and near optimal doped HTc superconductors) [4], as well as spin (URu_2Si_2) [5, 6] and charge density wave transitions (hole doped HTc) [7]. Recently, measuring specific heat and magnetization of a superconductor Mo_3Sb_7 with $T_c = 2.2$ K we have discovered an anomaly at $T^* = 50$ K, which has been ascribed to spin-gap formation due to the Mo–Mo spin dimerization [8]. The investigated compound crystallizes in the cubic Ir_3Ge_7-type structure. The unit cell of Mo_3Sb_7 is characterized by three orthogonal alternating stacks of the magnetic Mo ions (–Mo–Mo–4Mo–Mo–Mo–) and sandwiched with 4Sb prisms. Remarkably, the distance Mo–Mo within the Mo–Mo pair (0.3 nm) is much shorter than those between the Mo and 4Mo block (0.46 nm) or between chains (0.52 nm). This kind of Mo arrangement in the unit cell prefers the intradimer interaction (e.g., within the Mo–Mo pair) to be dominating, and at low temperatures a singlet state due to Mo–Mo spin dimerization would be expected. Very recently, Okabe *et al* [9] reported μSR data collected in longitudinal geometry. The reported data are consistent with the occurrence of spin-singlet state. The nature of the anomaly at 50 K was investigated by Koyama *et al* [10] and Tabata *et al* [11]. The authors pointed to the tetragonal lattice symmetry lowering and a long-range order of spin-singlet dimers below T^*. In this work, based on the muon spin relaxation (μSR) and inelastic neutron scattering (INS) data of superconducting Mo_3Sb_7 and its phonon reference Ru_3Sn_7 we give strong evidence for the spin pseudogap opening below $T^* = 50$ K. Our experiments indicate that this phase transition has an electronic/magnetic nature and an energy pseudogap of ∼150 K.

2. Experimental methods

Mo_3Sb_7 was prepared from Mo and Sb (purity 99.95% from Alfa Aesar) by solid-state reaction. The components were mixed in a stoichiometric ratio and sealed in an evacuated quartz tube. The ampoule was annealed at 750 °C for one week. The product was then powdered, pressed into pellets and annealed again for one week at 750 °C in an evacuated quartz ampoule. The purity, homogeneity and crystal structure of the sample were checked by x-ray diffraction. The lattice parameter of the investigated sample was refined in the Rietveld analysis using the WinPLOTR program [12]. The refinements of the x-ray data yield a lattice parameter $a = 0.9551(1)$ nm, in good agreement with that previously reported by Dashjav *et al* for a single crystal (0.9559 nm) [13]. The purity of the sample was also checked by a scanning electron microscope Phillips SEM 515 and an energy dispersive x-ray spectrometer PV9800 by collecting several spectra at various locations across the surface of a sintered pellet. The compositions determined by EDX Mo: 29.2 ± 3 at.% and Sb: 70.8 ± 3 at.% are close to the ideal composition Mo:Sb = 3:7. No impurity phase within the experimental error is observed in the EDX spectra. The superconductivity of the sample was corroborated by specific heat [14], and by muon spin rotation measurements [15].

Single crystals of Ru_3Sn_7 were grown using a tin-flux method. A mixture of Ru (purity at. 99.99%) and Sn (at. 99.999%) with the atomic ratio Ru:Sn = 1:12 was placed in an evacuated quartz ampoule and was heated with a heating rate of 15 °C h^{-1} up to 800 °C and kept at this temperature for 24 h, followed by cooling down to room temperature with a step of 10 °C h^{-1}. Excess Sn was removed by etching in HCl. The obtained single crystals with typical dimensions $0.1 \times 0.1 \times 0.2$ mm^3 were examined by a scanning electron microscope Phillips SEM 515 and an energy dispersive x-ray spectrometer PV9800. The room temperature x-ray powder diffraction data of pulverized crystals, indicated the sample to be single phase crystallizing in the cubic Ir_3Ge_7-type structure. The lattice parameter determined from least-squares refinements was $a = 0.9349$ nm, in good agreement with previous reported [16]. No magnetic contribution to magnetization, electrical resistivity and specific heat of the compound was established. From these two latter properties we deduced an Einstein ($\Theta_E = 100$ K) and two Debye temperatures ($\Theta_{D1} = 185$ K and $\Theta_{D2} = 298$ K) [17].

For μSR measurements, pulverized samples of Mo_3Sb_7 and Ru_3Sn_7, each of 5 g, were mixed with diluted GE varnish and attached onto a high purity silver (>4N) holder of 30 mm diameter and 1 mm thick. The μSR measurements were carried out using MuSR spectrometer installed at ISIS facility of the Rutherford Appleton Laboratory, Chilton, UK, where pulses of muons are produced every 20 ms with a FWHM of 70 ns. Muons are implanted into the sample, after which they decay with a half-life of 2.2 μs into positrons, which are emitted preferentially in the direction of the muon spin axis. These positrons are detected and time stamped in the detectors, which are positioned before, 'F', and after, 'B', the sample. The muon relaxation function $G_z(t)$ is obtained using the counts in F and B detectors as $G_z(t) = (N_F(t) - \alpha N_B(t))/(N_F(t) + \alpha N_B(t))$, where α is a calibration constant. The measurements were performed in zero-field longitudinal geometry over the temperature range 5–250 K. In order to examine the electronic nature of relaxation, muon data for Mo_3Sb_7 were additionally collected with a longitudinal field (LF) of 5 mT. A LF mode was used to decouple the nuclear dipolar field.

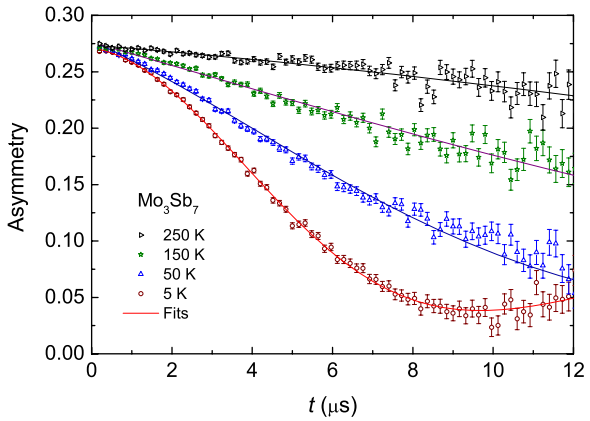

Figure 1. Zero-field μSR data for Mo_3Sb_7 at selected temperatures. The lines show the fits to the data.

Inelastic neutron scattering measurements were carried out on a 50 g pulverized sample of Mo_3Sb_7 and 10 g of Ru_3Sn_7 using the time-of-flight high energy transfer (HET) spectrometer at Rutherford Appleton Laboratory, Chilton, UK. The samples were wrapped in a thin Al foil sachet with a dimension of about $40 \times 40 \times 1$ mm^3 and attached to the cold finger of a closed cycle cryostat. The measurements were carried out at 5, 100, 200 and 300 K with selected incident neutron energy of 23, 60, 100, 200 and 500 meV.

3. Results and discussion

In figure 1 we show four example muon depolarization curves of Mo_3Sb_7, measured below T^*, at T^* and well above dimerization temperature T^*. The depolarization behaviour at all temperatures cannot be described by the standard static Kubo–Toyabe function:

$$G_{KT}(\sigma_{KT}, t) = \tfrac{1}{3} + \tfrac{2}{3}(1 - \sigma_{KT}^2 t^2)\exp(-\tfrac{1}{2}\sigma_{KT}^2 t^2), \quad (1)$$

where σ_{KT} is the nuclear depolarization rate [18]. To satisfactorily describe the experimental data, one needs to incorporate an exponential function $\exp(-\lambda t)$, describing the dynamically fluctuating internal fields at the muon site. So, we have analysed the data using the function:

$$G_z(\sigma_{KT}, \lambda, t) = A\exp(-\lambda t)G_{KT}(\sigma_{KT}, t) + A_{bg}, \quad (2)$$

where A and A_{bg} are the asymmetry contributions from the muons stopping within the sample and silver holder. It would also be possible to analyse the data with a dynamic Kubo–Toyabe, which models a diffusing muon. However, the fits to the μSR spectra are not as good as those using equation (2). Also, the process of forming a dimer means that the two

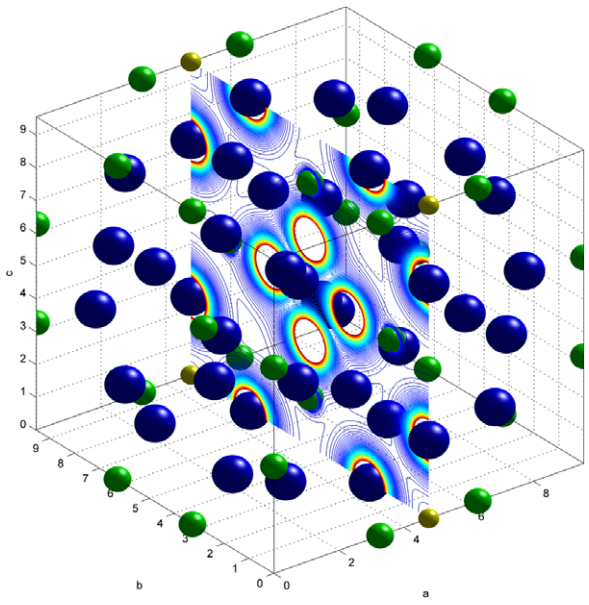

Figure 2. The crystallographic unit cell of Mo_3Sb_7 (Mo atoms at 16e, Sb atoms at 12d and 16f) and the most probable muon localization site (1/2, 0, 0). The smallest balls (yellow) are the muons, the middle-sized balls represent the Mo atoms and the biggest denote the Sb atoms.

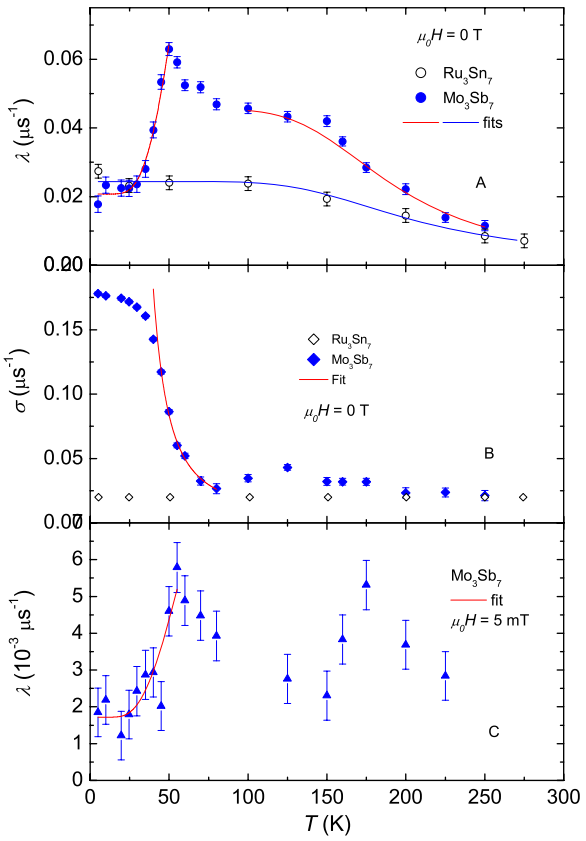

Figure 3. Figure (A) shows the temperature dependence of the electronic contribution to the relaxation rate and the lines are fits to the data. Figure (B) shows the temperature dependence of the nuclear contribution. The final figure (C) is the temperature dependence of the muon depolarization rate in an applied field of 5 mT. Again the line is a fit to the data.

relaxation phenomena are independent and therefore should be treated as such. Note that a similar procedure of fit was used by Koyama *et al* [10]. Fits to the spectra, shown in figure 1 as solid lines, have been obtained as follows. First we have determined the parameters A, λ and σ_{KT} and kept A_{bg} to be constant at all temperatures measured. As a result we found that the $A(T)$ of Ru_3Sn_7 practically shows no significant temperature dependence, while $A(T)$ of Mo_3Sb_7 exhibits different slopes in two temperature ranges; above T^*, the asymmetry weakly decreases with increasing temperature and below T^* there is a drop in the asymmetry. However, this drop is rather small, since the ratio $(A(50\ \mathrm{K}) - A(5\ \mathrm{K}))/A(50\ \mathrm{K})$ amounts to 0.028 only. This observation may indicate a little muon fraction of about 2.8% presumably associated with those muons depolarizing in the local magnetic field arising from the Mo spin dimers. Due to a negligible change in $A(T)$ of Mo_3Sb_7, in the following fitting we have kept constant A and A_{bg}, and from the fits we have determined the parameters λ and σ_{KT} as a function of temperature, as shown in figure 3.

As can be seen from figure 3, the temperature dependence of $\sigma(T)$ for Ru_3Sn_7 is weakly changed with temperature. This behaviour implies that the muon is static in this compound and therefore, one assumes that the magnetic field at the muon site is given by the sum of dipolar contributions:

$$\sigma_{KT}^2 = \frac{1}{6} I(I+1) \frac{8}{3} \left(\frac{\mu_0 \hbar}{4\pi} \gamma_\mu \gamma_n \right)^2 \left(1 + \frac{3}{8} \frac{I + 1/2}{I(I+1)} \sum_{i=1}^{N} \frac{1}{r_i^6} \right), \quad (3)$$

where I is the nuclear spin and γ_n is the gyromagnetic ratio of the nucleus [19]. Fitting of the data at 5 K to equation (3), we are able to identify the site (1/2, 0, 0), where the muons most likely stop at. More details of the calculation technique can be found in [20]. Assuming that structural distortion at 50 K does not significantly change the position of the Mo atoms and the muon is also static in Mo_3Sb_7, a similar procedure of the fitting has been treated for the nuclear depolarization rate of Mo_3Sb_7 at 5 K. From the fit results we can infer the most possible muon localization site is also (1/2, 0, 0) in Mo_3Sb_7 (see figure 2).

The obvious feature of figure 1 is that there is a clear difference between that below T^* and those above T^*. This difference results in strong temperature dependence of the parameters λ and σ_{KT} shown in figure 3. As far as the $\lambda(T)$ and $\sigma_{KT}(T)$-curves of Ru_3Sn_7 and Mo_3Sb_7 are concerned (figures 3(A) and (B)), we see that the superconducting Mo_3Sb_7 shows unusual behaviour around 50 K. In general, the muon relaxation rate is related to the local field $\langle B_{loc} \rangle$ and correlation time τ_c as $\lambda = \gamma_\mu \langle B_{loc}^2 \rangle \tau_c$. In a non-magnetic compound like Ru_3Sn_7 or in the paramagnetic state of Mo_3Sb_7, $\langle B_{loc}^2 \rangle$ does not show a large temperature variation, thus we may assume that the dynamic effect seen in the μSR data of these compounds is due to either spin–lattice relaxation or to thermally activated muon motion. These processes are associated with the correlation time τ_c of the interaction between muons and the Mo/Ru spins. One may take $\tau_c^{-1} = \tau_{ther}^{-1} + \tau_{sl}^{-1}$, where the motion rate is assumed to be $\tau_{ther}^{-1} = n_0 \exp(-E_{ther}/k_B T)$ and the spin–lattice relaxation

rate is assumed to follow the Korringa relation $\tau_{sl}^{-1} = KT$, and n_0, E_{ther}/k_B and K are constants [21]. It turns out that the best fit to the data is obtained with $n_0 = 2.22 \times 10^{-9}$ s, $E_{ther}/k_B = 850$ K and $K \approx 0$ for Ru_3Sn_7, and $n_0 = 3.34 \times 10^{-9}$ s, $E_{ther}/k_B = 975$ K and $K \approx 0$ for Mo_3Sb_7 (see the solid lines in figure 3(A)). The value of the activation gap appears to be comparable to those of Au and Cu alloys doped with Gd^{3+} and Er^{3+}, i.e. about 1350 K and 550 K, respectively [22]. The contribution of spin–lattice relaxation to the dynamic process of the investigated compounds seems to be negligible. It is clear from figure 3(A) that the muon relaxation data of Mo_3Sb_7 for $T < 50$ K could not be described by the change of a muon motion alone as for Ru_3Sn_7. This means that the second moment of the magnetic field distribution $\langle B_{loc}^2 \rangle$, and spin–spin correlation time τ_{ss} in addition to τ_{ther} and τ_{sl}, must be substantial. Accordingly, the pronounced feature observed T^* demonstrates the existence of various relaxation rate components in different temperature ranges, below and above T^*. As we have found in the magnetic susceptibility and specific heat [8], the temperature range below 50 K corresponds to the dimer state, thus the opening of the spin pseudogap may accompany a rapid drop in the relaxation rate λ. The temperature dependence of $\lambda(T)$ below 50 K can be well reproduced by an exponential function $\lambda(T) \propto \exp(-\Delta/k_BT)$ with $\Delta/k_B = 150(8)$ K, and is illustrated by the solid line in figure 3(A). Note that the observed pseudogap value agrees quite well with those deduced from the magnetic susceptibility (145 K) and heat capacity data (113 K) [8].

Looking at figure 3(B) we found no temperature dependence of σ_{KT} for Ru_3Sn_7, meaning that the data can be attributed entirely to the depolarization of the muon due to static Ru nuclear moments. On the other hand, it is remarkable that $\sigma_{KT}(T)$ of Mo_3Sb_7 shows a significant increase near 50 K. This behaviour indicates the appearance of internal fields due to short-range static magnetic correlations of the Mo spins. We interpret the fields to be originated from the formation of spin dimers. The data between 40 and 80 K can be fitted to thermally activated behaviour $\sigma_{KT}(T) = \sigma_{KT,0} \exp(E_a/k_BT)$ with an activation energy $E_a/k_B = 155(6)$ K and $\sigma_{KT,0} = 0.0037\ \mu s^{-1}$. Due to possible thermally activated motion, a motional narrowing process may yield an activation energy. However, in our opinion this scenario below 100 K is unlikely, because the dynamics of the thermally activated muon in Mo_3Sb_7 and Ru_3Sn_7 should be similar, and the activation energy for the muons in these compounds was found to be ∼900 K, i.e., of almost one order of magnitude higher than E_a/k_B. Moreover, the field spread caused by the nuclear dipole leads to a large Gaussian depolarization (∼0.18 μs^{-1}), compared to a slower dynamics due to the muon motion with the relaxation rate ∼0.025 μs^{-1} only. Thus, the temperature dependence of $\sigma_{KT}(T)$ and $\lambda(T)$ provide unambiguous evidence that a pseudogap with an energy of about 150 K opens up below 50 K. Figure 3(B) shows also a broad maximum around 125 K in the σ_{KT}-curve of Mo_3Sb_7. This may be related to two competing fractions of relaxing muons, one due to thermally activated muons and the other, due to short-range magnetic interactions between the Mo^{5+} ions, are electronic in nature.

In order to ascertain the origin of the exponential depolarization we measured the LF μSR at a longitudinal field of 5 mT. The obtained data are presented in figure 3(C). In this LF configuration, the nuclear dipolar relaxation is quenched ($G_{KT}(\sigma_{KT}, t) = 1$) and with the naked eye sharp maxima are seen in $\lambda_{LF}(T)$ at 50 and at 175 K. Again, below 50 K the relaxation rate is well fitted by the exponential function: $\lambda_{LF} = \lambda_0 + A \exp(-\Delta/k_BT)$ with $\lambda_0 = 1.7 \times 10^{-3}\ \mu s^{-1}$, $A = 0.053\ \mu s^{-1}$ and $\Delta/k_B = 150(10)$ K. Although the data show some decoupling, the dynamic behaviour of $\lambda(T)$ remains. This fact means that the observed hyperfine coupling between muons and the Mo spins is independent of nuclear dipolar fields. In other words, the observation brings new evidence that the short-range order around 170 K and an energy pseudogap opening at 50 K are of electronic/magnetic origin. We would like to note that the change in LF relaxation explains a small drop in $A(T)$ below T^*. An important observation in our study is that the relaxation rate does not vanish but persists at a finite value as temperature tends to 0 K. The non-zero residual relaxation in the LF relaxation was observed also by Tabata *et al* [11]. In the motional narrowing limit, the relaxation rate of the muon spins is approximated by $\lambda_{LF} = \frac{2(\gamma_\mu \mu_0 H)^2 \nu}{\nu^2 + (\gamma_\mu \mu_0 H)^2}$ with $\gamma_\mu/2\pi = 135.5$ MHz T^{-1}, $\mu_0 H$ is the applied strength of the longitudinal field and ν is the electronic fluctuation rate [23]. Taking $\mu_0 H = 5$ mT and $\lambda_0 = 1.7 \times 10^{-3}\ \mu s^{-1}$ we derive the frequency $\nu \sim 2 \times 10^{10}\ s^{-1}$. In a magnetic system with the spin S, the relaxation is normally correlated with the exchange interaction J via the relation: $\nu = \frac{2JS}{\hbar}$ [24]. If we put the residual frequency of $2 \times 10^{10}\ s^{-1}$ we get $J/k_B = 0.15$ K, indicating that the residual relaxation is not due to either intra- (J_0) or interdimer (J') exchange interactions, since these latter have exchange integrals $J_0/k_B \sim 150$ K and $J'/k_B \sim 720$ K [8], i.e. of two orders of magnitude larger. Thus, the proper nature of the residual relaxation rate is not established at this stage. Possible origins are either due to a static magnetic ordering of very small Mo moments in the normal state or due to quantum fluctuations at $T = 0$ K. However, these proposed mechanisms need stronger support from future investigations. Recently, we have found evidence of interplay between a spin density wave and superconductivity from the measurement of electrical resistivity $\rho(T)$ and magnetization $M(T)$ under hydrostatic pressure [32] and also from electron tunnelling spectroscopy [33]. The SDW characteristic as an upturn in $\rho(T)$ and antiferromagnetic peak in $M(T)$-curves occurs below 6.5 K, and correspondingly a V-like minimum in the differential conductance dI/dV versus V curve, manifesting the presence of a pseudogap in the DOS, is observed at 4.2 K. The SDW scenario is consistent with the electron band structure calculation, where a Fermi surface nesting has been found [8].

Figure 4 shows the inelastic neutron scattering spectra at higher momentum transfer (high-Q) and lower momentum transfer (low-Q) of Ru_3Sn_7 and Mo_3Sb_7 measured at 5 K with incident neutron energy $E_i = 60$ meV. It is clear from the figure that the spectral shape at high-Q, of Ru_3Sn_7 and Mo_3Sb_7 is nearly similar. This observation suggests the phonon spectra of these compounds are not so much different. For Ru_3Sn_7 one identifies one asymmetric broad inelastic peak of phonon

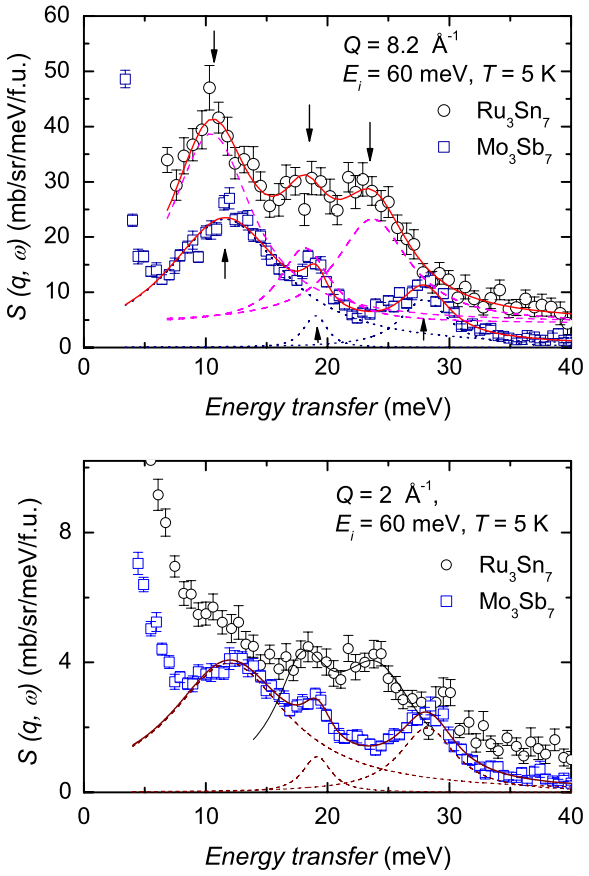

Figure 4. The constant Q-scans of the inelastic neutron scattering at 5 K with an incident energy of 60 meV for Ru_3Sn_7 and for Mo_3Sb_7. The upper panel represents data for $Q = 8.2$ Å and the lower panel for 2 Å. The lines are Lorentzian functions and the arrows indicate the centre of excitations.

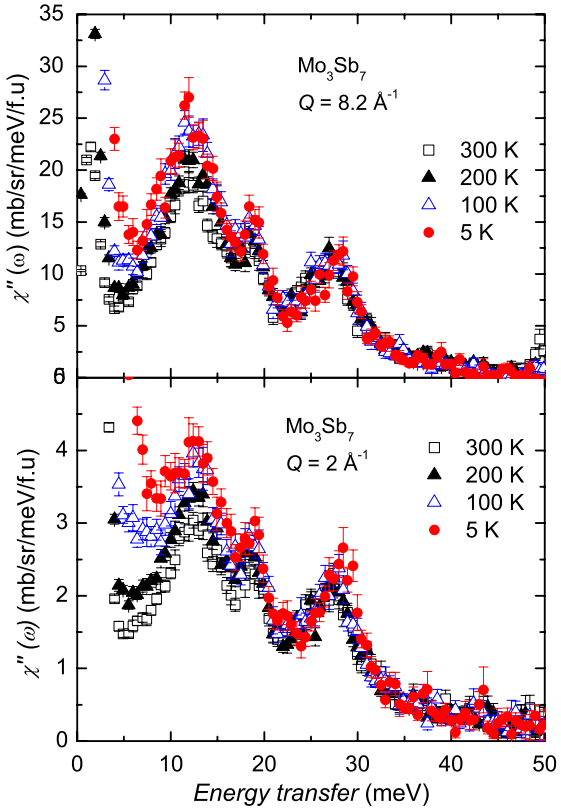

Figure 5. Local dynamic susceptibility of Mo_3Sb_7 with an incident energy of 60 meV collected at several selected temperatures. The upper panel represents data for $Q = 8.2$ Å and the lower panel for 2 Å.

density of states (PDOS) at around 11 meV and a flat structure between 18 and 23 meV in the high-Q spectrum. These INS spectra can be well reproduced by the Lorentzian response function with a centre at 10.57, 18.1 and 23.7 meV and a corresponding half width 8.0, 4.9 and 7.2 meV. The result of the fitting is shown as dashed lines in the upper panel. At low-Q spectrum (lower panel), the flat structure between 18 and 23 meV splits on two clear peaks. These three excitations coincide well to an Einstein (Θ_E = 100 K) and two Debye modes (Θ_{D1} = 185 K and Θ_{D2} = 298 K), derived from the specific heat and electrical resistivity data. The spectrum of Mo_3Sb_7 shows also Lorentzian type excitations. Three inelastic peaks located around 11.6, 19.0 and 27.9 meV with half width 11.4, 1.7 and 4.5 meV can be obtained from the fit (see the dotted lines in the upper panel). Recently, Wiendlocha *et al* performed phonon spectrum calculation [25]. The authors found three phonon peaks located at 2.8, 4.4 and 6 THz, thus, in very good agreement with our observation. Note the fact that the calculations were done for the cubic structure, therefore, the tetragonal distortion clearly does not significantly influence the phonon spectrum of Mo_3Sb_7.

Special attention should be paid to the remarkable difference between the spectra of Ru_3Sn_7 and Mo_3Sb_7 at lower momentum transfer (bottom panel), where the magnetic contribution (if it exists) should be dominating. In contrast to the behaviour of Ru_3Sn_7, all three peaks around 12, 19 and 28 meV for Mo_3Sb_7 persist still. This observation may indicate that there is some magnetic scattering or some change in the phonon density of state in Mo_3Sb_7 at low temperatures. Support of the magnetic contribution to the peak at 12.2 meV was found when one converts the temperature dependent magnetic structure factor $S(Q, \omega)$ to dynamic susceptibility $\chi''(Q, \omega)$ by multiplying the Bose population factor $[1 - \exp(-\hbar\omega/k_BT)]$, i.e., $\chi''(Q, \omega) = [1 - \exp(-\hbar\omega/k_BT)]S(Q, \omega)$. If the observed total response in Mo_3Sb_7 was entirely due to phonon scattering, then $\chi''(Q, \omega)$, should be temperature independent as $\chi''(Q, \omega)/Q^2$ represents PDOS. Otherwise, any change in $\chi''(Q, \omega)$ with temperature implies a dominant contribution of the magnetic response. The energy transfer dependencies of the dynamic susceptibility $\chi''(Q, \omega)$ of Mo_3Sb_7 at measured temperatures are shown in figure 5. At high-Q the excitations for Mo_3Sb_7 at ∼19 and ∼28 meV are basically phononic since they do not practically change with temperature, while the dynamic response at ∼12 meV should partly consist of a magnetic contribution. At low-Q, the magnetic excitation has clearly been observed at ∼12 meV. There is a weak additional contribution at ∼19 and ∼28 meV. We believe that the change in the $\chi''(Q, \omega)$ with temperature is associated with some kind of an electronic/magnetic nature of the phase transition at T^*. The essential question that now arises is what is

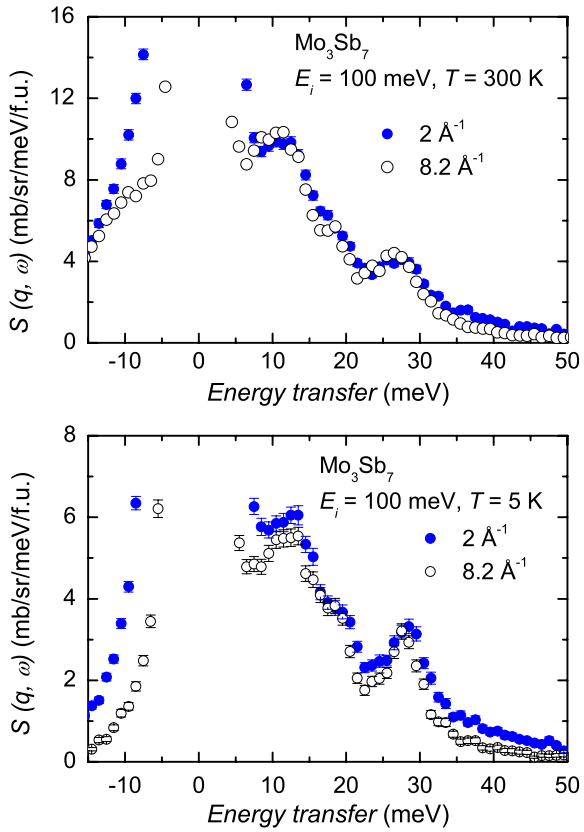

Figure 6. The constant Q-scans of the inelastic neutron scattering of Mo_3Sb_7 with an incident energy of 100 meV collected at 300 K (upper panel) and at 5 K (lower panel). The HQ data were normalized to LQ at 28 meV.

the nature origin of these scattering peaks. To follow the temperature dependence of excitation near 11–15 meV and near 24–32 meV, we compare the inelastic neutron scattering spectra of Mo_3Sn_7 collected at high-Q and low-Q, and at 300 K and at 5 for other incident neutron energy E_i = 100 meV in figure 6. At room temperature, the energy of the peaks is practically independent of the momentum transfer. Considering the peak at 29 meV, one sees a better defined structure for this peak at low temperature than at high temperature. Obviously, due to spin dimer formation and the lattice distortion we suppose that this behaviour could reflect a mixed mode consisting of magnetic and phononic. Regarding the excitation around 12 meV, one recognizes an extra contribution at the low-Q, indicative of magnetic origin. The energy of this peak (12.2 meV $\sim$ 142 K) has a similar value to the pseudogap obtained in muon measurement ($\sim$150 K), proving the consistency of the gapped nature of the transition at T^*.

4. Discussion and conclusions

Before discussing the connection between the observed spin pseudogap and superconductivity in Mo_3Sb_7 one considers the possible physical origin of the existence of the energy pseudogap $\sim$150 K. First, one may consider a lattice distortion [9–11], usually resulting in a spin-Peierls-type singlet ground state. In this scenario, the LF relaxation is expected to increase below the phase transition, as found for some spin-Peierls systems [26, 27]. This is not the case for Mo_3Sb_7, where a slowing down of the relaxation occurs. In the case of the spin dimer gap, as we have proposed in [8], the ground state is expected to be non-magnetic and relaxation should be due to nuclear dipolar relaxation only. Actually, in the applied LF mode for Mo_3Sb_7 we have still observed a muon residual relaxation, indicating electronic/magnetic origin of the phase transition.

For the studied compound Mo_3Sb_7, crystallizing in the cubic Ir_3Ge_7-type structure, structural instability can be expected to play an important role in the electron–phonon coupling, as was found in A15 superconductors [28]. Due to structural instability accompanied with a lattice distortion [9–11], some phonon mode softening can contribute to an enhancement of the electron–phonon. On the other hand, as theoretical calculations [25] and our experimental INS data indicated a good consistency in the phonon spectrum for the cubic structure is found. So the phonon mode softening due to the distortion is negligible. Moreover, our μSR data point out the spin pseudogap in Mo_3Sb_7 is of electronic nature and the relaxation in the gap state is governed by low energy excitations with a finite residual relaxation rate. In terms of electronic mechanisms, non-phonon pairing owing to plasmons or excitons is possible. In principle, in the system consisting of heavy and light mass electrons, just as suggested in Mo_3Sb_7 [8], the heavier mass electrons can be screened by the light mass electrons. As a consequence, an acoustic plasmon mode can be formed, which can act like a phonon in conventional BCS theory [29]. An alternative mechanism of the superconductivity is excitonic interaction [30]. Low energy excitations in Mo_3Sb_7 detected by the μSR measurement may be regarded as electron–hole-like excitations. In the existing theory for high-Tc cuprates the low-lying electronic excitations are referred to as holons and spinons and the superconductivity is realized via a condensation of holons pairs [31]. Another aspect of the electronic mechanism which has to be taken into account is spin correlation since in the dimer state of Mo_3Sb_7 there is competition between interdimer and intradimer Mo-spins interactions. Finally, there is a possible close relationship between SDW and superconductivity in Mo_3Sb_7. Recently, the measurements of both electrical resistivity and magnetization under pressure [32] and electron tunnelling spectroscopy [33] have indicated a SDW ordering in the normal state. The existence of a small residual relaxation rate and weak magnetic INS excitations around 12.5 meV at 5 K, indicating a static magnetic ordering or quantum fluctuations, might support the SDW ordering scenario.

In conclusion, we have determined the probable muon localization site in the unit cell and phonon spectra for Ru_3Sn_7 and Mo_3Sb_7. Based on the μSR and INS data, we found a spin pseudogap with an energy $\sim$150 K, appearing at $T^* = 50$ K in superconducting Mo_3Sb_7. We established that the phase transition at T^* is of electronic/magnetic nature. The present experiments together with magnetic susceptibility and specific heat data previously reported indicate that Mo_3Sb_7 possesses multiple transition properties like some unconventional high-Tc and heavy-fermion superconductors do. However, whether

structural instability, electronic excitations below T^* and/or SDW ordering below 6.5 K act as a proper trigger for the electron pairing mechanism in Mo_3Sb_7 is an open issue and the definitive interpretation for the relationship between spin pseudogap and superconductivity would require further detailed studies. To shed some insight on this relationship, experiments searching for magnetic resonance in the superconducting state of Mo_3Sb_7 are under way.

Acknowledgment

The work was supported by the Polish Ministry of Science and Higher Education through the research grants N202 082/0449.

References

[1] See, for instance Coleman P 2001 *Nature* **410** 320
[2] Kitaoka Y, Kawasaki S, Mito T and Kawasaki Y 2005 *J. Phys. Soc. Japan* **74** 186
[3] Saxena S S, Agarwal P, Ahilan K, Grosche F M, Haselwimmer R K W, Steiner M J, Pugh E, Walker I R, Julian S R, Monthoux P, Lonzarich G G, Huxley A, Sheikin I, Braithwaite D and Flouquet J 2000 *Nature* **406** 587
[4] Orenstein J and Millis A J 2000 *Science* **288** 468
[5] Palstra T T M, Menovsky A A, van den Berg J, Dirkmaat A J, Kess P H, Niewenhuys G J and Mydosh J A 1985 *Phys. Rev. Lett.* **55** 2727
[6] Maple M B, Chen J W, Dalichaouch Y, Kohara T, Rossel C, Torikachvili M S, McElfresh M W and Thompson J D 1986 *Phys. Rev. Lett.* **56** 185
[7] LeBoeuf D, Doiron-Leyraud N, Levallois J, Daou R, Bonnemaison J-B, Hussey N E, Balicas L, Ramshaw B J, Liang R, Bonn D A, Hardy W N, Adachi S, Proust C and Taillefer L 2007 *Nature* **450** 533
[8] Tran V H, Miiller W and Bukowski Z 2008 *Phys. Rev. Lett.* **100** 137004
[9] Okabe H, Akimitsu J, Takeshita S, Miyazaki M, Hiraishi M and Kadono R 2009 *Physica* B **404** 743
[10] Koyama T, Yamashita H, Takahashi Y, Kohara T, Watanabe I, Tabata Y and Nakamura H 2008 *Phys. Rev. Lett.* **101** 126404
[11] Tabata Y, Koyama T, Kohara T, Watanabe I and Nakamura H 2009 *Physica* B **404** 746
[12] Roisnel T and Rodriguez-Carvajal J 2009 *Program WinPLOTR* http://www-llb.cea.fr/winplotr/winplotr.htm
[13] Dashjav E, Szczepenowska A and Kleinke H 2002 *J. Mater. Chem.* **12** 345
[14] Tran V H, Miiller W and Bukowski Z 2008 *Acta Mater.* **56** 5694
[15] Tran V H, Hillier A D, Adroja D T and Bukowski Z 2008 *Phys. Rev.* B **78** 172505
[16] Chakoumakos B C and Mandrus D 1998 *J. Alloys Compounds* **281** 157
[17] Tran V H and Miiller W 2009 *Acta. Phys. Pol.* A **115** 83
[18] Kubo R and Toyabe T 1967 *Magnetic Resonance and Relaxation* ed R Blinc (Amsterdam: North-Holland)
[19] Schenck A 1985 *Muon Spin Rotation* (Bristol: Hilger)
[20] Hillier A D, Adroja D T, Giblin S R, Kockelmann W, Rainford B D and Malik S K 2007 *Phys. Rev.* B **76** 174439
[21] Abragam A 1961 *The Principles of Nuclear Magnetism* (London: Oxford University Press)
[22] Brown J A, Heffner R H, Hutson R L, Kohn S, Leon M, Olson C E, Schillaci M E, Dodds S A, Estle T L, Vanderwater D A, Richards P M and McMasters O D 1981 *Phys. Rev. Lett.* **47** 261
[23] Hayano R S, Lemura Y I, Imazato J, Nishida N, Yamazaki T and Kubo R 1979 *Phys. Rev.* B **20** 850
[24] Watanabe I, Wada N, Yano H, Okuno T, Awaga K, Ohira S, Nishiyama K and Nagamine K 1998 *Phys. Rev.* B **58** 2438
[25] Wiendlocha B, Tobola J, Sternik M, Kaprzyk S, Parlinski K and Oleś A M 2008 *Phys. Rev.* B **78** 060507R
[26] Aïn M, Blundell S J, Lord J, Jegoudez J and Revcolevschi A 2000 *Physica* B **281/282** 648
[27] Blundell S J, Pratt F L, Pattenden P A, Kurmoo M, Chow K H, Takagi S, Jestädt Th and Hayes W 1997 *J. Phys.: Condens. Matter* **9** L119
[28] Testardi L R 1975 *Rev. Mod. Phys.* **47** 637
[29] Entin-Wohlman O and Gutfreund H 1984 *J. Phys. C: Solid State Phys.* **17** 1071
[30] Allender D, Bray J and Bardeen J 1973 *Phys. Rev.* B **7** 1020
[31] Gimm T-H, Lee S-S, Hong S-P and Suck Salk S-H 1999 *Phys. Rev.* B **60** 6324
[32] Tran V H, Khan R T, Wiśniewski P and Bauer E 2009 *Phys. Rev. Lett.* submitted
(Tran V H, Khan R T, Wiśniewski P and Bauer E 2009 arXiv:0907.5530v1)
[33] Tran V H, Batkova M, Batko I, Pribulova Z and Bukowski Z 2009 *Proc. Int. Conf. on Quantum Criticality and Novel Phases (Dresden, Aug. 2009)*; *Phys. Status Solidi* b at press